

# Strain-Induced Room-Temperature Ferromagnetic Semiconductors with Giant Anomalous Hall Effect in Two-Dimensional $\text{Cr}_2\text{Ge}_2\text{Se}_6$

Xue-Juan Dong<sup>1</sup>, Jing-Yang You<sup>1</sup>, Bo Gu<sup>2,3,\*</sup> and Gang Su<sup>1,2,3†</sup>

<sup>1</sup> School of Physical Sciences, University of Chinese Academy of Sciences, Beijing 100049, China

<sup>2</sup> Kavli Institute for Theoretical Sciences, University of Chinese Academy of Sciences, Beijing 100190, China

<sup>3</sup> CAS Center for Excellence in Topological Quantum Computation,  
University of Chinese Academy of Sciences, Beijing 100190, China

(Dated: January 29, 2019)

By density functional theory calculations, we predict a stable two-dimensional (2D) ferromagnetic semiconductor  $\text{Cr}_2\text{Ge}_2\text{Se}_6$ , where the Curie temperature  $T_c$  can be dramatically enhanced beyond room temperature by applying a few percent strain. In addition, the anomalous Hall conductivity in 2D  $\text{Cr}_2\text{Ge}_2\text{Se}_6$  and  $\text{Cr}_2\text{Ge}_2\text{Te}_6$  is predicted to be comparable to that in ferromagnetic metals of Fe and Ni, and is an order of magnitude larger than that in diluted magnetic semiconductor  $\text{Ga}(\text{Mn},\text{As})$ . The enhanced  $T_c$  in  $\text{Cr}_2\text{Ge}_2\text{Se}_6$  by strain can be understood by superexchange interaction with two mechanisms. One is the enhanced direct antiferromagnetic coupling between Te/Se and Cr, and the other is the enhanced ferromagnetism due to decreased  $3d$  orbital occupation number  $n_d$  of Cr away from the critical value, at which the nonmagnetic state is obtained. Our finding highlights the microscopic mechanisms to obtain the room temperature ferromagnetic semiconductors by strain.

Combining magnetism and semiconductor enables the development of magnetic semiconductors, a promising way to realize spintronic applications based on use of both charge and spin degrees of freedom in electronic devices [1, 2]. The highest Curie temperature of the most extensively studied magnetic semiconductor  $(\text{Ga},\text{Mn})\text{As}$  has been  $T_c = 200$  K [3], still far below room temperature. The room temperature ferromagnetic semiconductors are highly required by applications. Recent advances in magnetism in two-dimensional (2D) van der Waals materials have provided a new platform for the study of magnetic semiconductors [4]. The Ising ferromagnetism with out-of-plane magnetization was observed in monolayer  $\text{CrI}_3$  in experiment with  $T_c = 45$  K [5]. The Heisenberg ferromagnetic state was obtained in 2D  $\text{Cr}_2\text{Ge}_2\text{Te}_6$  in experiment with  $T_c = 28$  K in bilayer  $\text{Cr}_2\text{Ge}_2\text{Te}_6$  [6], where the corresponding bulk was known as a layered ferromagnet with spin along  $c$  axis and  $T_c = 61$  K in experiment [7]. A large remanent magnetization with out-of-plane magnetic anisotropy was recently reported in experiment in the 6-nm film of  $\text{Cr}_2\text{Ge}_2\text{Te}_6$  on a topological insulator  $(\text{Bi},\text{Sb})_2\text{Te}_3$  with  $T_c = 80$  K [8]. The magnetic structure in monolayer  $\text{CrI}_3$  and  $\text{Cr}_2\text{Ge}_2\text{Te}_6$  was recently discussed in terms of Kitaev interaction [9]. The ferromagnetism with high  $T_c$  was also reported in experiment in the monolayer  $\text{VSe}_2$  [10] and  $\text{MnSe}_2$  [11]. Despite the relatively small number of monolayer ferromagnetic materials realized in experiment, predicting promising candidates by first principles calculations can provide reliable reference for experiments [12]. Researchers have also studied possible 2D ferromagnetic materials by machine learning [13] and high-throughput calculations [14].

Several methods are used to control the magnetic states in these recently discovered 2D materials. By tuning gate voltage, the switching between antiferromagnetic and ferromagnetic states in bilayer  $\text{CrI}_3$  was obtained in

experiment [15]. Using gate voltage, the enhancement of ferromagnetism in 2D  $\text{Fe}_3\text{GeTe}_2$  was observed in recent experiment [16]. In 2D transition metal dichalcogenides, which are non-magnetic, the strain is used to modify the optical and electronics properties [17]. The effect of strain is studied to affect the ferromagnetism in monolayer  $\text{Cr}_2\text{Ge}_2\text{Te}_6$  [18] and  $\text{CrX}_3$  ( $X = \text{Cl}, \text{Br}, \text{I}$ ) [19]. The electric field effect was discussed in experiment in magnetic multilayer  $\text{Cr}_2\text{Ge}_2\text{Te}_6$  [20].

In this paper, by density functional theory calculations we predict a stable 2D ferromagnetic semiconductor  $\text{Cr}_2\text{Ge}_2\text{Se}_6$ . We find that  $T_c = 144$  K in  $\text{Cr}_2\text{Ge}_2\text{Se}_6$ , which can be enhanced to  $T_c = 326$  K by applying 3% strain, and  $T_c = 421$  K by 5% strain. On the other hand,  $T_c$  in 2D semiconductor  $\text{Cr}_2\text{Ge}_2\text{Te}_6$  is about 30 K in our calculation, close to the value of  $T_c = 28$  K in recent experiment [6]. In addition, the anomalous Hall conductivity in 2D  $\text{Cr}_2\text{Ge}_2\text{Se}_6$  and  $\text{Cr}_2\text{Ge}_2\text{Te}_6$  is predicted to be comparable to that in ferromagnetic metals of Fe and Ni [21–23], and is an order of magnitude larger than that in diluted magnetic semiconductor  $\text{Ga}(\text{Mn},\text{As})$  [24, 25]. The strain is found to have two effects in terms of superexchange interaction to enhance the  $T_c$  in  $\text{Cr}_2\text{Ge}_2\text{Se}_6$ . One is the enhanced direct antiferromagnetic coupling between Se and Cr, and the other is the enhanced ferromagnetic coupling by decreased  $3d$  orbital occupation number  $n_d$  of Cr away from the critical value, at which the nonmagnetic state is obtained. Our finding highlights the microscopic mechanisms to obtain the room temperature magnetic semiconductors by strain.

The density functional theory (DFT) calculations are done by the Vienna *ab initio* simulation package (VASP) [26]. The spin-polarized calculation with projector augmented wave (PAW) method, and general gradient approximations (GGA) in the Perdew-Burke-Ernzerhof (PBE) exchange correlation functional are used. To-

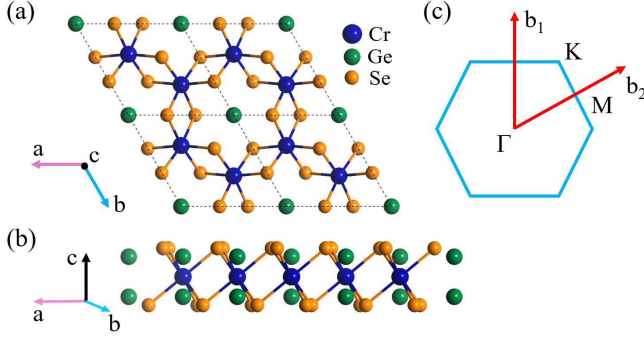


FIG. 1. Crystal structure of  $\text{Cr}_2\text{Ge}_2\text{Se}_6$  of (a) top view in a-b plane and (b) side view in a-c plane. The two-dimensional Brillouin zone is shown in (c).

tal energies are obtained with k-grids  $9 \times 9 \times 1$  by Mohnkhorst-Pack approach. The lattice constants and atom coordinates are optimized with the energy convergence less than  $10^{-6}$  eV and the force less than  $0.01$  eV/Å, where a large vacuum of  $20$  Å is used to model a 2D system. The phonon calculations are performed with density functional perturbation theory (DFPT) by the PHONOPY code [27]. Size of the supercell is  $3 \times 3 \times 1$ , where the displacement is taken by  $0.01$  Å.

For the on-site Coulomb interaction  $U$  of Cr ion, parameter  $U$  is chosen to test as 3, 4, and 5 eV, which are the reasonable  $U$  values for  $3d$  transition metal insulators [28]. We found that the lattice slightly increases by 0.2% with these  $U$  parameters. When we study the magnetism in 2D  $\text{Cr}_2\text{Ge}_2\text{Te}_6$  with these values, we obtained the ferromagnetic ground state for  $U = 4$  eV, and antiferromagnetic ground state for  $U = 5$  eV. Because the ferromagnetic state is obtained in 2D  $\text{Cr}_2\text{Ge}_2\text{Te}_6$  in experiment [6], we fixed the parameter  $U = 4$  eV in our following calculations for 2D  $\text{Cr}_2\text{Ge}_2\text{Te}_6$  and  $\text{Cr}_2\text{Ge}_2\text{Se}_6$ .

Based on the DFT results, the Curie temperature is calculated by using the Monte Carlo simulations [18, 19] based on the 2D Ising model, where a  $60 \times 60$  supercell was adopted, and  $10^5$  steps are performed for every temperature to acquire the equilibrium. The anomalous Hall conductivity is calculated with Wannier90 code [29] and WannierTools code [30].

*Crystal Stability*— We study the stability of the 2D new material  $\text{Cr}_2\text{Ge}_2\text{Se}_6$ . We propose this material guided by the recently reported 2D material  $\text{Cr}_2\text{Ge}_2\text{Te}_6$  in experiment, and we replace Te by Se. The crystal structure of  $\text{Cr}_2\text{Ge}_2\text{Se}_6$  is shown in Fig. 1 (a) for top view and 1 (b) for side view, where the space group number is 162 (P-31m). The structure is obtained by the fully relaxed calculation. The optimized lattice constant of 2D  $\text{Cr}_2\text{Ge}_2\text{Se}_6$  is calculated as  $6.413$  Å, which is smaller than the lattice constant  $6.8275$  Å of  $\text{Cr}_2\text{Ge}_2\text{Te}_6$  in experiment. It is reasonable because Se has a smaller radius than Te. We examine the stability in terms of phonon spectrum, where the Brillouin zone is shown in Fig. 1(c).

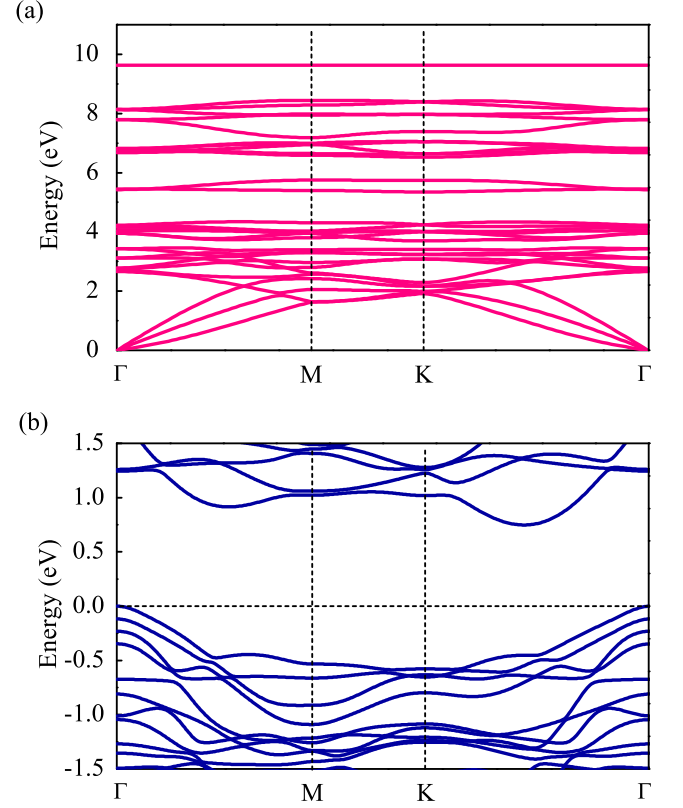


FIG. 2. (a) Phonon spectrum and (b) electron band structure of two-dimensional  $\text{Cr}_2\text{Ge}_2\text{Se}_6$ , obtained by the density functional theory (DFT) calculations.

As shown in Fig. 2(a), there is no imaginary frequency in the phonon dispersion near  $\Gamma$  point. It predicts that the crystal structure of monolayer  $\text{Cr}_2\text{Ge}_2\text{Se}_6$  is stable. In addition, the electronic band structure of  $\text{Cr}_2\text{Ge}_2\text{Se}_6$  is shown in Fig. 2(b). An indirect band gap of  $0.748$  eV is observed, and monolayer  $\text{Cr}_2\text{Ge}_2\text{Se}_6$  is a semiconductor.

*Magnetic States*— To study the magnetic ground state of 2D  $\text{Cr}_2\text{Ge}_2\text{Se}_6$ , we examine the possible states with paramagnetic, ferromagnetic and antiferromagnetic configurations. The calculations reveal that the energy of the paramagnetic state is 6 eV higher than the ferromagnetic and antiferromagnetic states. Fig. 3(a) shows four possible magnetic states of 2D  $\text{Cr}_2\text{Ge}_2\text{Se}_6$ : ferromagnetic (FM) state, antiferromagnetic (AFM) Néel state, AFM stripe state, and AFM zigzag state. The calculations show that the FM state is the most stable state, and the energy difference between the FM and the AFM configuration is more than 30 meV as listed in Table I. Furthermore, as shown in Fig. 3(b), the calculations show that the lowest energy of ferromagnetic state is obtained when the magnetization direction is perpendicular to the two-dimensional materials, with magnetic anisotropy energy of  $0.32$  meV per unit cell of  $\text{Cr}_2\text{Ge}_2\text{Se}_6$ . As listed in Table I, the calculation shows that for 2D  $\text{Cr}_2\text{Ge}_2\text{Se}_6$ , the spin momentum of Cr atom is  $3.4 \mu_B$ , and the occupation

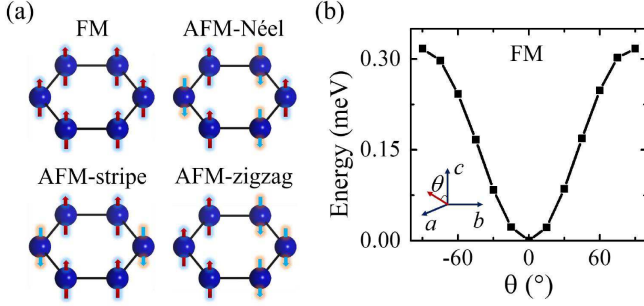


FIG. 3. (a) Four possible states for two-dimensional  $\text{Cr}_2\text{Ge}_2\text{Se}_6$ : ferromagnetic (FM) state, antiferromagnetic (AFM) Néel state, AFM stripe state, and AFM zigzag state. Balls denote Cr atoms, and arrows denote spins. (b) Total energy as a function of angle  $\theta$  for the FM state, obtained by the DFT calculations.

TABLE I. For 2D semiconductors  $\text{Cr}_2\text{Ge}_2\text{Te}_6$ ,  $\text{Cr}_2\text{Ge}_2\text{Se}_6$ , and  $\text{Cr}_2\text{Ge}_2\text{Se}_6$  with 5% strain, DFT results of total energy of ferromagnetic state  $E^{\text{FM}}$ , total energy of antiferromagnetic state  $E^{\text{AFM}}$ , Curie temperature  $T_c$ , 3d orbital occupation number  $n_d$ , spin ( $S$ ) and orbital ( $L$ ) momentum of Cr atom, and bond length  $d_{\text{Cr}-\text{Te}/\text{Se}}$ .

DFT	$\text{Cr}_2\text{Ge}_2\text{Te}_6$	$\text{Cr}_2\text{Ge}_2\text{Se}_6$	
		no strain	5% strain
$E^{\text{FM}}(\text{eV})$	-89.1376	-97.3460	-96.5658
$E^{\text{AFM}}(\text{eV})$	-89.1309	-97.3135	-96.4710
$E^{\text{AFM}}-E^{\text{FM}}(\text{meV})$	6.7	32.5	98.8
$T_c(\text{K})$	30	144	421
$n_d(\text{Cr})$	4.043	3.976	3.951
$S(\mu_B)(\text{Cr})$	3.586	3.404	3.487
$L(\mu_B)(\text{Cr})$	-0.018	-0.076	-0.105
$d_{\text{Cr}-\text{Te}/\text{Se}}(\text{\AA})$	2.827	2.64	2.697

number of Cr 3d orbitals is 3.976.

**Curie Temperature  $T_c$** — The  $T_c$  can be estimated by the Monte Carlo simulation based on a 2D Ising model. The exchange coupling parameter is estimated as the total energy difference of ferromagnetic and antiferromagnetic states  $E^{\text{AFM}}-E^{\text{FM}}$  as listed in Table I, which was obtained by the DFT calculations. The obtained normalized magnetization as function of temperature is shown in Fig. 4 (a). The experimental result of magnetization for  $\text{Cr}_2\text{Ge}_2\text{Te}_6$  is taken from temperature-dependent Kerr rotation of bilayer  $\text{Cr}_2\text{Ge}_2\text{Te}_6$  with  $T_c = 28$  K [6]. The calculated Curie temperature is  $T_c = 30$  K for the monolayer  $\text{Cr}_2\text{Ge}_2\text{Te}_6$ , which is close to the experimental value. It is noted that for simplicity the Ising model is applied in our Monte Carlo simulation, while the Heisenberg model with magnetic anisotropy was suggested in experiment [6]. In addition, the estimated Curie temperature  $T_c$  could be even larger by using the mean field approximation [14]. The calculated Curie temperature for monolayer  $\text{Cr}_2\text{Ge}_2\text{Se}_6$  is  $T_c = 144$  K, which is about 5 times

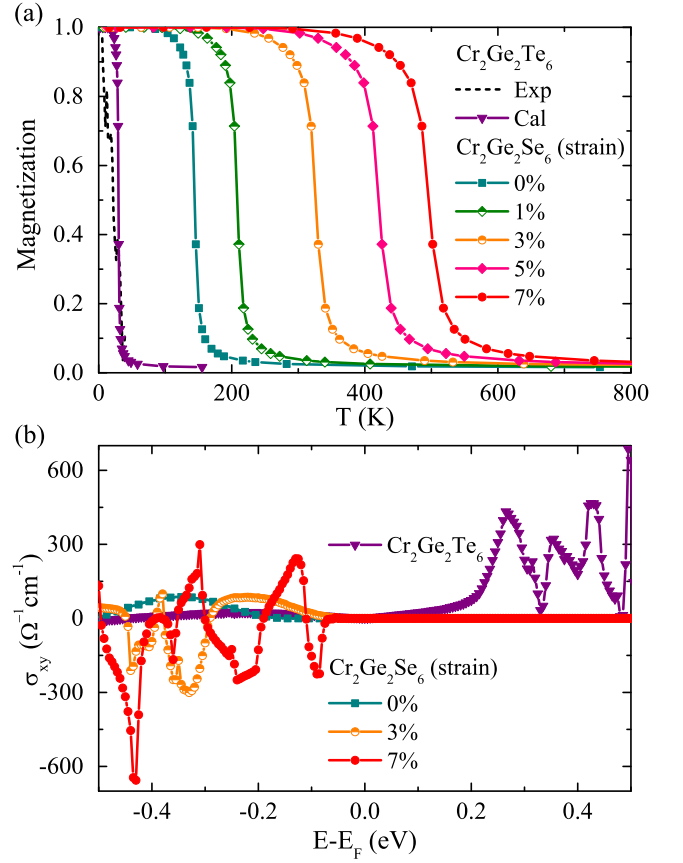


FIG. 4. For two-dimensional  $\text{Cr}_2\text{Ge}_2\text{Te}_6$  and  $\text{Cr}_2\text{Ge}_2\text{Se}_6$  with different strains, (a) the normalized magnetization as a function temperature, and (b) the anomalous Hall conductivity as a function of energy. The experimental result of  $\text{Cr}_2\text{Ge}_2\text{Te}_6$  is taken from Ref. [6]. The calculation results are obtained by the DFT calculations and Monte Carlo simulations.

higher than the  $T_c = 30$  K for monolayer  $\text{Cr}_2\text{Ge}_2\text{Te}_6$  by the Monte Carlo simulation. More interestingly, the Curie temperature can be enhanced to  $T_c = 326$  K by applying 3% strain, and  $T_c = 421$  K with 5% strain, as shown in Fig. 4(a). Our result predicts that monolayer  $\text{Cr}_2\text{Ge}_2\text{Se}_6$  by applying a few percent strain can be a promising candidate for room-temperature ferromagnetic semiconductor.

**Anomalous Hall Conductivity**— As the magnetization direction is out-of-plane with an easy axis along  $c$  direction in 2D  $\text{Cr}_2\text{Ge}_2\text{Te}_6$  and  $\text{Cr}_2\text{Ge}_2\text{Se}_6$ , it is interesting to study the anomalous Hall conductivity due to the Berry curvature of band structure. By the DFT calculations, the results are shown in Fig. 4(b). The magnitude of anomalous Hall conductivity  $\sigma_{xy}$  for the p-type  $\text{Cr}_2\text{Ge}_2\text{Se}_6$  and n-type  $\text{Cr}_2\text{Ge}_2\text{Te}_6$  can be as large as  $4 \times 10^2 (\Omega \text{ cm})^{-1}$ . This value is comparable to the  $\sigma_{xy}$  in some ferromagnetic metals, such as  $\sigma_{xy} = 7.5 \times 10^2$  in bcc Fe [21, 22], and  $\sigma_{xy} = 4.8 \times 10^2 (\Omega \text{ cm})^{-1}$  in fcc Ni [23] due to the Berry curvature of band structures. More

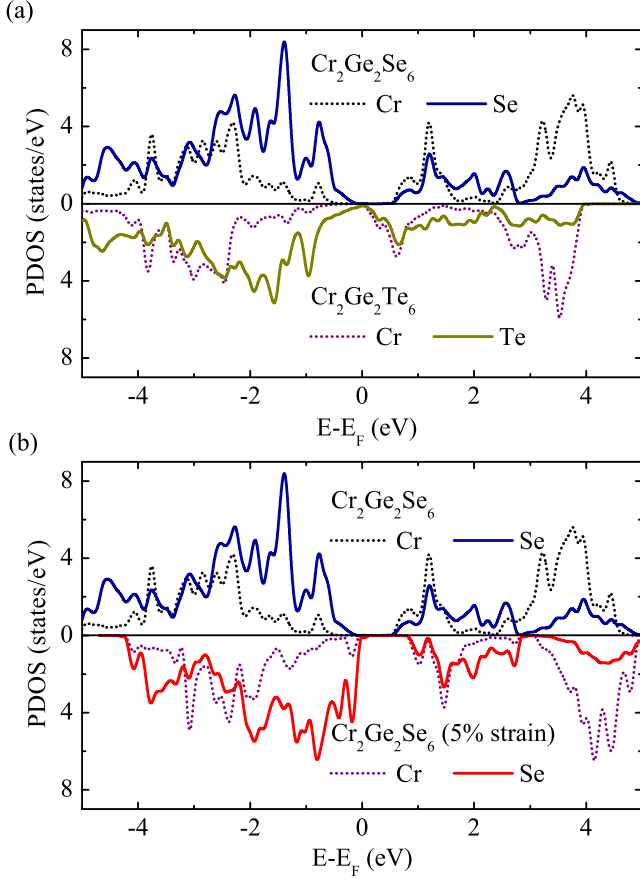


FIG. 5. Partial density of state (PDOS) for two-dimensional (a)  $\text{Cr}_2\text{Ge}_2\text{Te}_6$  and  $\text{Cr}_2\text{Ge}_2\text{Se}_6$ , and (b)  $\text{Cr}_2\text{Ge}_2\text{Te}_6$  without and with 5% strain, obtained by the DFT calculations.

importantly, the estimated  $\sigma_{xy}$  in 2D magnetic semiconductors  $\text{Cr}_2\text{Ge}_2\text{Te}_6$  and  $\text{Cr}_2\text{Ge}_2\text{Se}_6$  is an order of magnitude larger than the  $\sigma_{xy}$  of classic diluted magnetic semiconductor  $\text{Ga}(\text{Mn},\text{As})$  [24, 25].

**Mechanisms of Enhanced  $T_c$** — The ferromagnetism in  $\text{Cr}_2\text{Ge}_2\text{Te}_6$  comes from the superexchange interaction [7, 20], which is also expected in  $\text{Cr}_2\text{Ge}_2\text{Se}_6$ . By the superexchange model, the  $\text{Cr}(3d)\text{-Te}(5p)/\text{Se}(4p)\text{-Cr}(3d)$  bond induces the indirect magnetic coupling between two Cr ions, bridged by the  $p$  orbitals of center Te/Se ion. There are two factors determining the superexchange interaction, one is the direct antiferromagnetic coupling between Te/Se and Cr, and the other is the  $3d$  orbital occupation number  $n_d$  of Cr.

As shown in Table I, the length of bond Se-Cr in  $\text{Cr}_2\text{Ge}_2\text{Se}_6$  is 2.64 Å, which is smaller than the value of 2.827 Å for the length of bond Te-Cr in  $\text{Cr}_2\text{Ge}_2\text{Te}_6$ . Because the shorter bond can induce stronger direct exchange coupling, the antiferromagnetic exchange coupling between Se-Cr in  $\text{Cr}_2\text{Ge}_2\text{Se}_6$  can be stronger than that between Te-Cr in  $\text{Cr}_2\text{Ge}_2\text{Te}_6$ . As a result, the stronger mediated ferromagnetic coupling between Cr

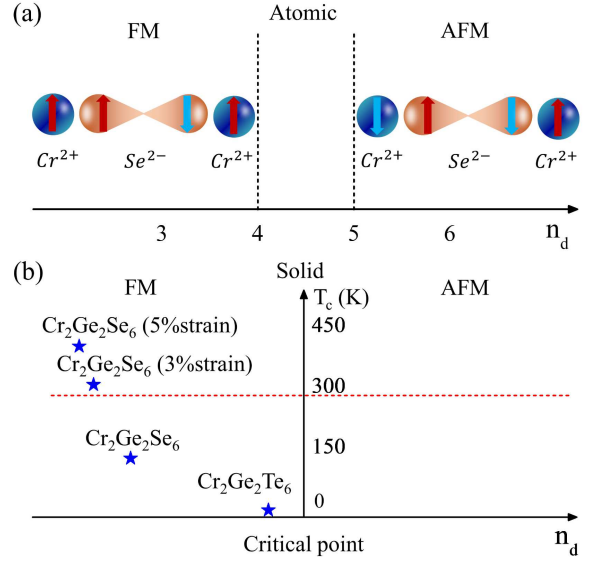


FIG. 6. (a) Schematic picture of superexchange. For  $d$  orbital occupation number  $n_d \leq 4$ , the  $\text{Cr}(3d)\text{-Se}(4p)\text{-Cr}(3d)$  system is ferromagnetic. For  $n_d \geq 5$ ,  $\text{Cr}(3d)\text{-Se}(4p)\text{-Cr}(3d)$  system is antiferromagnetic. (b) Schematic picture of our argument to understand the enhanced  $T_c$  in  $\text{Cr}_2\text{Ge}_2\text{Se}_6$  based on superexchange picture. See text for details.

ions, and the higher  $T_c$  in  $\text{Cr}_2\text{Ge}_2\text{Se}_6$  are expected. But this mechanism cannot be applied to explain the strain-enhanced  $T_c$  in  $\text{Cr}_2\text{Ge}_2\text{Se}_6$ . As shown in Table I, the length of bond Se-Cr in  $\text{Cr}_2\text{Ge}_2\text{Se}_6$  with 5% strain is 2.697 Å, larger than the value 2.64 Å of Se-Cr in  $\text{Cr}_2\text{Ge}_2\text{Se}_6$  without strain. The same argument gives the result that the  $T_c$  in  $\text{Cr}_2\text{Ge}_2\text{Se}_6$  should decrease with strain, while the opposite results of  $T_c$  are obtained in calculation as shown in Table I.

In fact, the antiferromagnetic coupling between the bond  $\text{Se}(4p)\text{-Cr}(3d)$  can be estimated from the partial density of state (PDOS) of Se and Cr. The direct exchange coupling between Se and Cr should be proportional to the product of the occupied PDOS of Se  $4p$  and Cr  $3d$  orbitals. By density functional theory calculations, the obtained PDOS for 2D  $\text{Cr}_2\text{Ge}_2\text{Te}_6$ ,  $\text{Cr}_2\text{Ge}_2\text{Se}_6$ , and  $\text{Cr}_2\text{Ge}_2\text{Se}_6$  with 5% strain are shown in Fig. 5. It is observed that the occupied PDOS of Cr  $3d$  orbital does not change so much, while the occupied PDOS of Se  $4p$  in  $\text{Cr}_2\text{Ge}_2\text{Se}_6$  is larger than that of Te  $5p$  in  $\text{Cr}_2\text{Ge}_2\text{Te}_6$  as shown in Fig. 5(a). So, the product of occupied PDOS of Cr( $3d$ ) and Se( $4p$ ) is larger than that of Cr( $3d$ ) and Te( $5p$ ), and the antiferromagnetic coupling between Se( $4p$ ) and Cr( $3d$ ) in  $\text{Cr}_2\text{Ge}_2\text{Se}_6$  should be larger than that in  $\text{Cr}_2\text{Ge}_2\text{Te}_6$ . The similar result is observed for the  $\text{Cr}_2\text{Ge}_2\text{Se}_6$  with and without strain as shown in Fig. 5(b), where the occupied PDOS of Se  $4p$  increase by strain, and thus the antiferromagnetic coupling between neighboring Se( $4p$ ) and Cr( $3d$ ) increases by strain.

The other factor affecting the superexchange is the  $3d$



orbital occupation number  $n_d$  of Cr. As shown in Fig. 6, we propose a mechanism based on  $3d$  orbital occupation number  $n_d$  of Cr. In the atomic limit, the superexchange gives the ferromagnetic coupling for  $n_d \leq 4$ , and antiferromagnetic coupling for  $n_d \geq 5$ , where  $n_d$  is  $d$  orbital occupation number of magnetic ion. We argue that a small  $T_c$  in  $\text{Cr}_2\text{Ge}_2\text{Te}_6$  suggests that the  $n_d$  in  $\text{Cr}_2\text{Ge}_2\text{Te}_6$  is close and below the critical value. At critical value of  $n_d$ , the nonmagnetic state is obtained. By strain,  $n_d$  in  $\text{Cr}_2\text{Ge}_2\text{Se}_6$  is decreased further away from the critical value, which makes  $T_c$  in  $\text{Cr}_2\text{Ge}_2\text{Se}_6$  dramatically enhanced. Our finding highlights a new way to control the magnetism with slightly tuning  $n_d$  for the materials with  $n_d$  close to the critical value.

In summary, by the DFT calculations we predict a stable 2D ferromagnetic semiconductor  $\text{Cr}_2\text{Ge}_2\text{Se}_6$ . We find the Curie temperature  $T_c$  of  $\text{Cr}_2\text{Ge}_2\text{Se}_6$  can be dramatically enhanced beyond room temperature by applying 3 % strain, which is much higher than the  $T_c = 28$  K in 2D  $\text{Cr}_2\text{Ge}_2\text{Te}_6$  in recent experiment. In addition, the anomalous Hall conductivity in 2D  $\text{Cr}_2\text{Ge}_2\text{Se}_6$  and  $\text{Cr}_2\text{Ge}_2\text{Te}_6$  is predicted to be an order of magnitude larger than that in diluted magnetic semiconductor Ga(Mn,As). Based on superexchange interaction, two mechanisms are found to be important to enhance the  $T_c$  in 2D  $\text{Cr}_2\text{Ge}_2\text{Se}_6$  by applying strain. One is the enhanced direct antiferromagnetic coupling between Se and Cr due to the increased partial density of state of Se( $4p$ ), and the other is the enhanced ferromagnetic coupling due to the decreased  $3d$  orbital occupation number  $n_d$  of Cr away from the critical value. Our finding highlights the microscopic mechanisms to obtain the room temperature ferromagnetic semiconductors by strain.

The authors acknowledge Q. B. Yan, Z. G. Zhu, and Z. C. Wang for many valuable discussions. BG is supported by NSFC (Grant No. Y81Z01A1A9) and UCAS (Grant No.110200M208). GS is supported in part by the the National Key R&D Program of China (Grant No. 2018FYA0305800), the Strategic Priority Research Program of CAS (Grant No. XDB28000000), and the NSFC (Grant No. 11834014).

---

\* gubo@ucas.ac.cn

† gsu@ucas.ac.cn

- [1] H. Ohno, *Science* **281**, 951 (1998).
- [2] T. Dietl, *Nat. Mater.* **9**, 965 (2010).
- [3] L. Chen, X. Yang, F. Yang, J. Zhao, J. Misuraca, P. Xiong, and S. von Molnár, *Nano Lett.* **11**, 2584 (2011).
- [4] K. S. Burch, D. Mandrus, and J.-G. Park, *Nature* **563**, 47 (2018).
- [5] B. Huang, G. Clark, E. Navarro-Moratalla, D. R. Klein, R. Cheng, K. L. Seyler, D. Zhong, E. Schmidgall, M. A. McGuire, D. H. Cobden, W. Yao, D. Xiao, P. Jarillo-Herrero, and X. Xu, *Nature* **546**, 270 (2017).
- [6] C. Gong, L. Li, Z. Li, H. Ji, A. Stern, Y. Xia, T. Cao, W. Bao, C. Wang, Y. Wang, Z. Q. Qiu, R. J. Cava, S. G. Louie, J. Xia, and X. Zhang, *Nature* **546**, 265 (2017).
- [7] V. Cartheaux, D. Brunet, G. Ouvrard, and G. Andre, *J. Phys.: Condens. Matter* **7**, 69 (1995).
- [8] M. Mogi, A. Tsukazaki, Y. Kaneko, R. Yoshimi, K. S. Takahashi, M. Kawasaki, and Y. Tokura, *APL Materials* **6**, 091104 (2018).
- [9] C. Xu, J. Feng, H. Xiang, and L. Bellaiche, *npj Comput. Mater.* **4**, 57 (2018).
- [10] M. Bonilla, S. Kolekar, Y. Ma, H. C. Diaz, V. Kalappattil, R. Das, T. Eggers, H. R. Gutierrez, M.-H. Phan, and M. Batzill, *Nat. Nanotechnol.* **13**, 289 (2018).
- [11] D. J. O'Hara, T. Zhu, A. H. Trout, A. S. Ahmed, Y. K. Luo, C. H. Lee, M. R. Brenner, S. Rajan, J. A. Gupta, D. W. McComb, and R. K. Kawakami, *Nano Lett.* **18**, 3125 (2018).
- [12] B. Shabbir, M. Nadeem, Z. Dai, M. S. Fuhrer, Q.-K. Xue, X. Wang, and Q. Bao, *Appl. Phys. Rev.* **5**, 041105 (2018).
- [13] T. D. Rhone, W. Chen, S. Desai, A. Yacoby, and E. Kaxiras, arXiv preprint arXiv:1806.07989 (2018).
- [14] H. Liu, J.-T. Sun, M. Liu, and S. Meng, *J. Phys. Chem. Lett.* **9**, 6709 (2018).
- [15] B. Huang, G. Clark, D. R. Klein, D. MacNeill, E. Navarro-Moratalla, K. L. Seyler, N. Wilson, M. A. McGuire, D. H. Cobden, D. Xiao, W. Yao, P. Jarillo-Herrero, and X. Xu, *Nat. Nanotechnol.* **13**, 544 (2018).
- [16] Y. Deng, Y. Yu, Y. Song, J. Zhang, N. Z. Wang, Z. Sun, Y. Yi, Y. Z. Wu, S. Wu, J. Zhu, J. Wang, X. H. Chen, and Y. Zhang, *Nature* **563**, 94 (2018).
- [17] R. Roldán, A. Castellanos-Gomez, E. Cappelluti, and F. Guinea, *J. Phys.: Condens. Matter* **27**, 313201 (2015).
- [18] X. Li and J. Yang, *J. Mater. Chem. C* **2**, 7071 (2014).
- [19] J. Liu, Q. Sun, Y. Kawazoe, and P. Jena, *Phys. Chem. Chem. Phys.* **18**, 8777 (2016).
- [20] W. Xing, Y. Chen, P. M. Odenthal, X. Zhang, W. Yuan, T. Su, Q. Song, T. Wang, J. Zhong, S. Jia, X. C. Xie, Y. Li, and W. Han, *2D Mater.* **4**, 024009 (2017).
- [21] Y. Yao, L. Kleinman, A. H. MacDonald, J. Sinova, T. Jungwirth, D. sheng Wang, E. Wang, and Q. Niu, *Phys. Rev. Lett.* **92**, 037204 (2004).
- [22] X. Wang, J. R. Yates, I. Souza, and D. Vanderbilt, *Phys. Rev. B* **74**, 195118 (2006).
- [23] X. Wang, D. Vanderbilt, J. R. Yates, and I. Souza, *Phys. Rev. B* **76**, 195109 (2007).
- [24] T. Jungwirth, J. Sinova, K. Y. Wang, K. W. Edmonds, R. P. Campion, B. L. Gallagher, C. T. Foxon, Q. Niu, and A. H. MacDonald, *Appl. Phys. Lett.* **83**, 320 (2003).
- [25] J. Sinova, T. Jungwirth, S.-R. E. Yang, J. Kučera, and A. H. MacDonald, *Phys. Rev. B* **66**, 041202 (2002).
- [26] G. Kresse and J. Furthmüller, *Phys. Rev. B* **54**, 11169 (1996).
- [27] A. Togo and I. Tanaka, *Scr. Mater.* **108**, 1 (2015).
- [28] S. Maekawa, T. Tohyama, S. E. Barnes, S. Ishihara, W. Koshihara, and G. Khaliullin, *Physics of Transition Metal Oxides* (Springer Berlin Heidelberg, 2004).
- [29] A. A. Mostofi, J. R. Yates, G. Pizzi, Y.-S. Lee, I. Souza, D. Vanderbilt, and N. Marzari, *Comput. Phys. Commun.* **185**, 2309 (2014).
- [30] Q. Wu, S. Zhang, H.-F. Song, M. Troyer, and A. A. Soluyanov, *Comput. Phys. Commun.* **224**, 405 (2018).